Research article

Effect of Carbonization Temperature on Physical Properties and Specific Capacitance of Activated Carbon Derived from Banana Stem and Its Application as Supercapacitor Electrodes

Paweena Dulyaseree[1]*, Hasanee Sama[1], Suraida Sada[1], Pundita Ukkakimapan[2], Visittapong Yordsri[3], Vichuda Sattayarut[2] and Winadda Wongwiriyapan[2]

[1]*Industrial Physics Program, Faculty of Science Technology and Agriculture, Yala Rajabhat University, Yala, Thailand*
[2]*College of Materials Innovation and Technology, King Mongkut's Institute of Technology Ladkrabang, Bangkok, Thailand*
[3]*National Metal and Materials Technology Center (MTEC), Pathum Thani, Thailand*

Abstract

In this work, activated carbons (ACs) for electrodes supercapacitor applications were successfully synthesized from banana stem. Banana is one of the popular fruits that is easy to grow and most parts of the plant can be used. However, banana cultivation generates a lot of wastes, especially from the stem. Thus, using banana stem as raw material for ACs was investigated. The synthesis of AC consisted of 2 processes; carbonization and activation. The advantage of a two-step synthesis was the low weight loss of charcoal. Firstly, the carbonization process was conducted by varying the temperature between 300-600°C, and then inorganic elements were removed by treatment with 1 M sulfuric acid. After that, activation was conducted at 720°C under an argon atmosphere. The electrochemical properties of banana stem-derived ACs (BCH-ACs) were studied using sodium sulfate as an electrolyte. The BCH-ACs carbonized at 400°C showed the highest performance with a specific capacitance of 55.45 Fg^{-1}, an energy density of 7.70 $Whkg^{-1}$ and a power density of 133.94 Wkg^{-1}. The highest specific capacitance of the BCH400-AC was likely due to the increase in the amount of oxygenated functional group, which facilitated the access of electrolyte ions into the electrode. These results suggest that banana stem can be used to synthesize ACs via carbonization at 400°C, and the ACs generated can be applied as electrode in supercapacitors.

---

*Corresponding author: E-mail: paweena.d@yru.ac.th

1. Introduction

The *Saba* banana is botanically known as part of Musa acuminate x balbisiana (ABB Group) and is a member of the Musaceae family. It is native to the three southern border provinces of Thailand, Malaysia and Indonesia. Banana is one of the popular fruits that is easy to grow, and most of its parts including the peel, stem, leaves, and fruit can be utilized [1-4]. Banana fruit crop production is estimated to be over 72.5 million tons per year, making it the fourth most significant fruit crop in the world [2]. After the banana fruit is mature and picked, the banana stem is chopped off and often discarded [1, 5, 6]. However, banana stem contains high lignin and cellulose, which are important starting materials for the synthesis of activated carbons (ACs) [7]. Biomass-derived ACs are widely utilized in energy storage device application [8-17], while also being used as catalyst supports [18, 19] and as adsorbents [20, 21].

Among energy storage (EC) devices, supercapacitors are situated in between dielectric capacitors and batteries Due to the unavoidable energy urgency coming from the limited supply of fossil fuels, ECs have been garnering growing attention. Because of its unique physical and chemical features, carbon has been used as an electrode material basis. Its excellent electrical conductivity and surface area make it a suitable material for supercapacitors because of its low production cost and controllable pore structure. Considering the high carbon content, AC has a large surface area and high porosity. AC microstructures are largely depending on the type of raw materials used. Improvements of electrode materials such as improving surface area and increasing oxygenated functional groups on carbon surfaces have been the primary focus of attempts to increase EC performance [22]. Normally, ACs can be synthesized in two steps: (i) a carbonization step to change the biomass into a carbonaceous structure via hydrothermal or pyrolysis and (ii) an activation step to form the pores in the carbon network by chemical or physical activation. The advantage of the two-step synthesis is a low weight loss of charcoal. Using banana stem as a raw material is a significant challenge.

In this study, the synthesis of ACs derived from banana stem at various carbonization temperature was investigated. The ACs were prepared in two steps; the first step was the carbonization process prepared by varying temeratures between 300-600°C, and the second step was the chemical activation at 720°C. The surface morphologies and electrochemical characteristics of the ACs derived from banana stem were examined. The ACs derived from banana stem at a carbonization temperature of 400°C showed the highest specific capacitance.

2. Materials and Methods

2.1 Syhthesis and characterization of banana stem-derived activated carbon

Fresh banana stem was obtained from Yala, one of three southern border provinces of Thailand, washed with water, and dried at 60°C overnight, and then ground into minute bits using a blender. The synthesis of ACs consisted of two processes; carbonization and activation. Firstly, carbonization process was conducted by varying temperature between 300-600°C for 120 min, with nitrogen flow rate of 0.5 Lmin^{-1} at a heating rate of 5°Cmin^{-1}. This was followed by the removal of inorganic components with 1 M sulfuric acid at 100°C for 180 min. Each sample was then continuously rinsed with deionized (DI) water until it reached its natural pH level and then dried at 110°C fovernight (hereafter referred to as BC). The BC was then mixed with sodium hydroxide (NaOH) at a ratio of 1:2.5 by weight, and then heated under nitrogen flow in a tubular furnace at 720°C for 60 min at a nitrogen flow rate of 5 Lmin^{-1}. Following the thermal activation, each sample was cleaned with DI water until its natural pH level was obtained, as described elsewhere (hereafter

referred to as BCH-AC) [14]. A scanning electron microscope (SEM, JEOL JSM-7800F) was used to examine the structure of the BCH samples, while a Raman spectrometer with a laser excitation wavelength of 532 nm (Thermo Scientific DXR SmartRaman) and a Fourier transform-infrared spectrometer were used to determine the functional groups present (FTIR, PerkinElmer Scientific, Spectrum Two FT-IR Spectrometer).

2.2 Electrode preparation and characterization of electrochemical properties

The electrode materials were a mixture of BCH-AC, carbon black and polytetrafluoroethylene (PTFE) at a weight ratio of 90:5:5, respectively. The materials were then crushed for 1 min at a pressure of 10 kN to create an electrode pellet with a diameter of 1 mm. The electrode material had a total mass loading of approximately 20 mg. A three-electrode setup was used for electrochmical measurement (Metrohm AUTOLAB PGSTAT 302). The working, counting and reference electrode used were BCH-AC, Pt sheet and Ag/AgCl electrodes, respectively. The electrolyte solution used was 1 M of sodium sulphate (Na_2SO_4). Using cyclic voltammetry (CV) with a potential range of 0.0-1.0 V at a scan rate of 5 mVs^{-1} and galvanostatic charge-discharge (CD) with a current density of 0.1 Ag^{-1}, the electrochemical properties of the samples were analyzed. The specific capacitance of the electrode materials in the three-electrode system (C_s) was caculated from CD curves using the following equations:

$$C_s = \frac{I \times \Delta t}{m \times \Delta v} \tag{1}$$

where $C_s, I, \Delta t$, and Δv are the specific capacitance of electrode material (Fg^{-1}), applied current (A), discharge time (s), the total loading mass of electrode pellets (g), respectively. Equations (2) and (3) were used to calculate the device's energy density (E, $Whkg^{-1}$) and power density (P, Wkg^{-1}).

$$E = \frac{1}{2} \times C_s \times \Delta V^2 \times \frac{1}{3.6} \tag{2}$$

$$P = \frac{E}{\Delta t} \times 3600 \tag{3}$$

3. Results and Discussion

Figure 1 shows SEM images of the BCH-ACs carbonized at different temperatures. The morphologies of BCH-AC showed higher amounts of broken structures and higher surface roughness with increasing temperature of carbonization. We characterized the crystallinity of the ACs using Raman spectroscopy with excitation using a 532 nm (2.33 eV) argon ion laser and a power of 5 mW. As shown in Figure 2, the Raman spectra consist of two characteristic peaks; a D-band at a Raman shift of $\sim$1336 cm^{-1} and a G-band at a Raman shift of $\sim$1567 cm^{-1}. The disordered carbon structure and sp3 hybridized carbon gave rise to the D-band, whereas the graphitic structure dominated by sp2 bonds gave rise to the G-band [23, 24]. The intensity ratio of the D-band to the G-band (I_D/I_G) may be used to assess defect locations in carbon structures [25, 26]. It was found that the I_D/I_G ratio decreased after the activation process, i.e. the I_D/I_G ratio of BC were 1.12, 1.15, 1.28 and 1.20 and the I_D/I_G ratio of BCH-AC were 0.93, 0.96, 0.97 and 0.98 for carbonization temperatures of 300, 400, 500 and 600°C, respectively. These results indicated a higher degree of
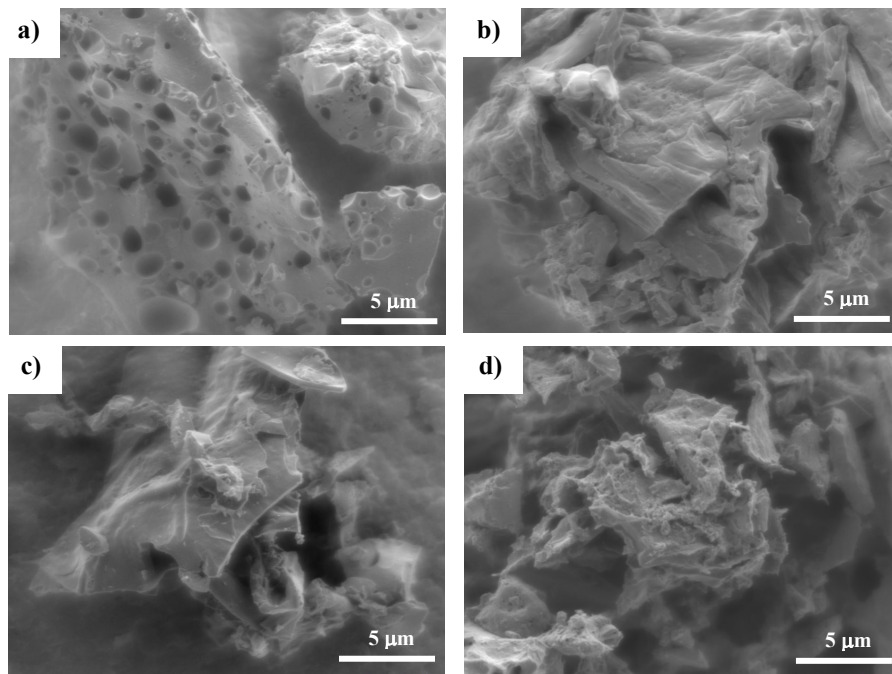
Figure 1. SEM images of (a) BCH300-AC, (b) BCH400-AC, (c) BCH400-AC, and (d) BCH500-AC
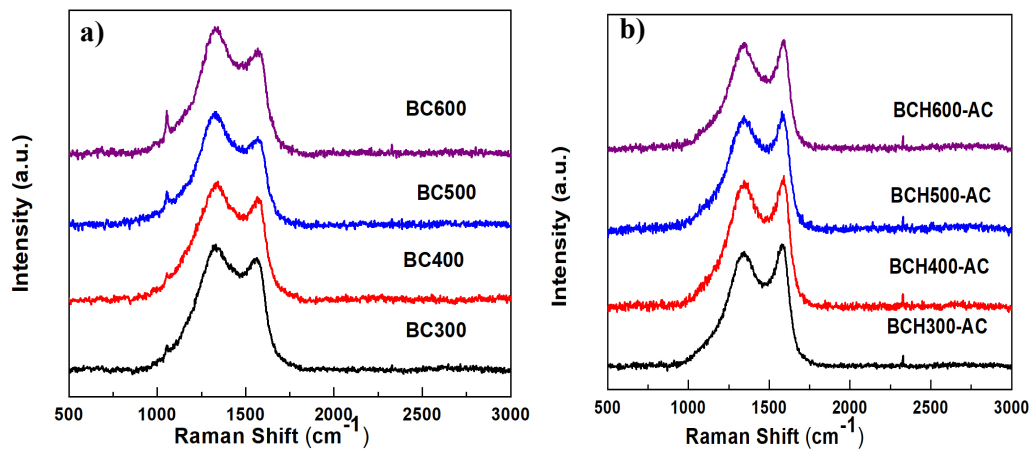

Figure 2. Raman spectra of (a) carbonization (BC) process, and (b) activation (BCH) process

graphitic structure, resulting from the decomposition of amorphous structures and organic components by the activation process.

The surface functional groups of BCH-ACs were also investigated by FT-IR. Figure 3 shows FT-IR spectra of BCH300-AC, BCH400-AC, BCH500-AC, and BCH600-AC. The stretching vibration of the hydroxyl (OH) group is represented by the broad peak at 2500-3300 cm^{-1}. The OH groups may from absorbed water, carboxylic acids and alcohols of cellulose, hemicellulose. The peak at ∼1514 cm^{-1} is attributed to the aromatic ring vibration (C=C) of lignin [27]. The peak at ∼1175 cm^{-1} is assigned to the stretching vibration of the C–O group of cellulose [28]. Interestingly, BCH400-AC showed a high level of the functional groups of aromatic rings and carbonyl groups. A high content of oxygenated functional groups may be beneficial for supercapacitor electrodes by improving of carbon surface wettability, and by taking part in the faradaic reaction, thereby increasing the specific capacitance [14, 29].
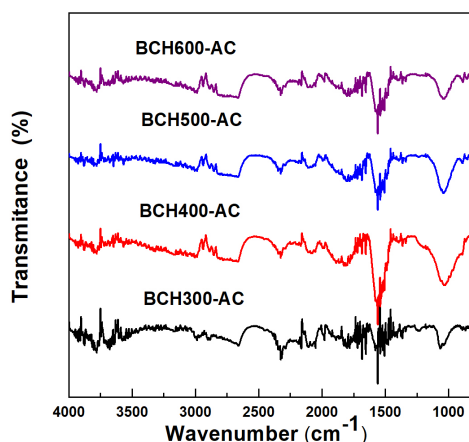

Figure 3. FT-IR spectra of BCH-ACs carbonized at different temperatures

Figure 4a shows the CV curves of different electrodes in a potential window range of 0.0-1.0 V at a scan rate of 5 mVs^{-1}. Electrical double-layer capacitors (EDLC) at the electrode-electrolyte interface had quasi-rectangular geometries. The BCH400-AC showed the largest area of CV curves, indicating the highest specific capacitance. Figure 4b shows CD curves in the 0.0-1.0 V potential range with a current density of 0.1 Ag^{-1}. All CD curves had a symmetric triangular form, indicating high electrochemical reversibility and the best supercapacitor characteristics [30]. BCH400-AC had a longer charge-discharge duration than other samples produced at different carbonization temperatures, indicating a greater specific capacitance. The values of the specific capacitance were observed to be in the following order: BCH400-AC (55.45 Fg^{-1}) > BCH500-AC (45.84 Fg^{-1}) > BCH600-AC (29.65 Fg^{-1})> BCH300-AC (25.95 Fg^{-1}). The calculated energy and power density of BCH300-AC, BCH400-AC, BCH500-AC, and BCH600-AC were approximately 3.60, 7.70, 6.37, and 4.12 $Whkg^{-1}$, and 117.93, 133.94, 127.32, and 123.54 Wkg^{-1}, respectively. The BCH400-AC showed the highest performance, energy density and power density. The BCH400-AC had the greatest specific capacitance due to an increase in the numbers of oxygenated functional groups, which allowed the electrolyte ions to easily enter the electrode materials. Table 1 shows the comparison of specific capacitance (C_s) of different electrode materials. The present study represents an improvement over some earlier works done and is comparable to previously published research materials.
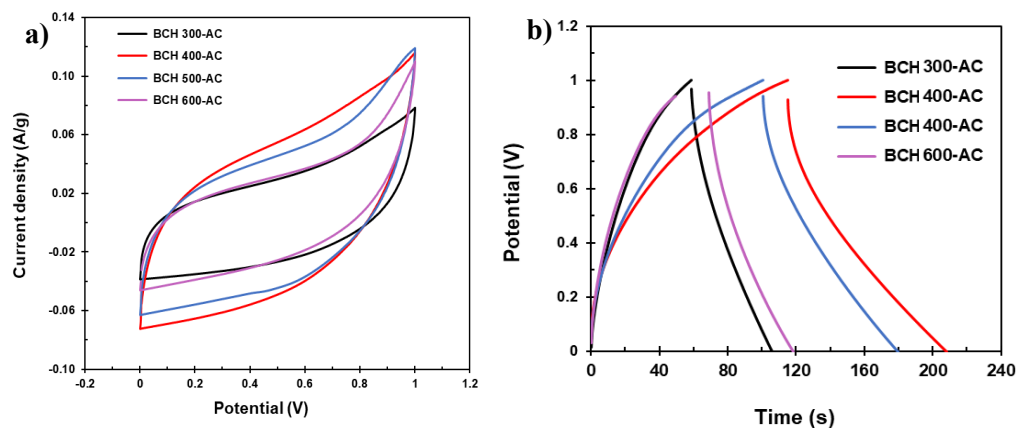
Figure 4. Electrochemical performance of the sample in 1 M Na_2SO_4 electrolyte. (a) CV curves at a scan rate of 5 mVs^{-1}, and (b) CD curves at a current density of 0.1 Ag^{-1}

Table 1. Comparison of specific capacitance (C_s) of different electrode materials

Electrode material	Specific capacitance (Fg^{-1})	Energy density ($Whkg^{-1}$)	Power density (Wkg^{-1})	References
Samanea saman leaves	179	35.3	542.3	[15]
Durian husk	145	32	316	[17]
Tobacco waste	148	2.6	52	[31]
Wheat straw	294	11	260	[32]
Pomelo peel	280	17.1	420	[33]
Aloe vera	200	40	150	[34]
Banana-peel	68	0.75	31	[35]
Banana-peel	155.5	7	250	[36]
Banana stem	55.45	7.70	133.94	This work

4. Conclusions

In summary, ACs derived from Saba banana stem were successfully synthesized. The best performance was that of BCH400-AC, which had a specific capacitance, energy and power density of 55.45 Fg^{-1}, 7.70 $Whkg^{-1}$ and 133.94 Wkg^{-1}, respectively. In the BCH400-AC, there was a rise in the amount of oxygenated functional groups, which made it easier for the electrolyte ions to access the electrode materials. These results suggest that banana stem can be used as a raw material for synthesis of ACs and can be applied as an electrode of supercapacitor.

5. Acknowledgements

References

[1] Li, K., Fu, S., Zhan, H., Zhan, Y. and Lucia, L., 2010. Analysis of the chemical composition and morphological structure of banana pseudo-stem. *BioResources*, 5, 576-585.

[2] Aziz, N.A.A., Ho, L-H., Azahari, B., Bhat, R., Cheng, L-H. and Ibrahim, M.N.M., 2011. Chemical and functional properties of the native banana (*Musaacuminata×balbisiana* Colla cv. Awak) pseudo-stem and pseudo-stem tender core flours. *Food Chemistry*, 128(3), 748-753.

[3] Sango, T., Cheumani, A.M., Duchatel, L., Marin, A., Kor, N.M. and Joly, N., 2018. Step-wise multi-scale deconstruction of banana pseudostem (*Musa acuminata*) biomass and morpho–mechanical characterization of extracted long fibres for sustainable applications. *Industrial Crops and Products*, 122, 657-668.

[4] Padam, B.S., Tin, H.S., Chye, F.Y. and Abdullah, M.I., 2014. Banana by-products: An under-utilized renewable food biomass with great potential. *Journal of Food Science and Technology*, 51, 3527-3545.

[5] Ahmad, T. and Danish, M., 2018. Prospects of banana waste utilization in wastewater treatment: A review. *Journal of Environmental Management*, 206, 330-348.

[6] Abdullah, N., Sulaiman, F., Miskam, M.A. and Taib, R.M., 2014. Characterization of banana (*Musa* spp.) pseudostem and fruit-bunch-stem as a potential renewable energy resource. *International Journal of Biological, Veterinary, Agricultural and Food Engineering*, 8, 712-716.

[7] Khalil, H.S.A., Alwani, M.S. and Omar, A.K.M., 2007. Chemical composition, anatomy, lignin distribution, and cell wall structure of Malaysian plant waste fibers. *BioResources*, 1(2), 220-232.

[8] Arie, A.A., Kristianto, H., Demir, E. and Cakan, R.D., 2018. Activated porous carbons derived from the Indonesian snake fruit peel as anode materials for sodium ion batteries. *Materials Chemistry and Physics,* 217, 254-261.

[9] Kurniawan, A., Suwandi, A.C., Lin, C.X., Ismadji, X.S. and Ong, L.K., 2012. A facile and green preparation of durian shell-derived carbon electrodes for electrochemical double-layer capacitors. *Progress in Natural Science: Materials International,* 22, 624-630.

[10] Chen, X., Zhang, J., Zhang, B., Dong, S. and Guo, X., 2017. A novel hierarchical porous nitrogen-dopedcarbon derived from bamboo shoot for high performance supercapacitor. *Scientific Reports,* 7, DOI: 10.1038/s41598-017-06730-x.

[11] Lee, D., Cho, Y.G., Song, H.K., Chun, S.J., Park, S.B. and Choi, D.H., 2017. Coffee-driven green activation of cellulose and its use for all-paper flexible supercapacitors. *ACS Applied Materials & Interfaces,* 9, 22568-22577.

[12] Chen, H., Yu, F., Wang, G., Chen, L., Dai, B. and Peng, S., 2018. Nitrogen and sulfur self-doped activated carbon directly derived from elm flower for high-performance supercapacitors. *ACS Omega.* 3, 4724-4732.

[13] Liang, T., Chen, C., Li, X. and Zhang, J., 2016. Popcorn-derived porous carbon for energy storage and CO_2 capture. *Langmuir,* 32, 8042-8049.

[14] Dulyaseree, P., Fujishige, M., Yoshida, I., Toya, Y., Banba, Y., Tanaka, S., Aoyama, T., Phonyiem, M., Wongwiriyapan, W., Takeuchi, K. and Endo, M., 2017. Nitrogen-rich green leaves of papaya and Coccinia grandis as precursors of activated carbon and their electrochemical properties. *RSC Advance,* 7, 42064-42072.

[15] Sattayarut, V., Wanchaem, T., Ukkakimapan, P., Yordsri, V., Dulyaseree, P., Phonyiem, M., Obata, M., Fujishige, M., Takeuchi, K., Wongwiriyapan, W., Endo, M., 2019. Nitrogen self-doped activated carbons via the direct activation of *Samanea saman* leaves for high energy density supercapacitors. *RSC Advance,* 9, 21724-21732.

[16] Ukkakimapan, P., Wanchaem, T., Yordsri, V., Sattayarut, V., Phonyiem, M., Fujishige, M., Takeuchi, K. and Wongwiriyapan, W., 2020. Investigation on electrochemical properties of sugarcane leaves-derived activated carbon by steam activation. *Solid State Phenomena,* 302, 63-70.

[17] Ukkakimapan, P., Sattayarut, V., Wanchaem, T., Yordsri, V., Phonyiem, M., Ichikawa, S., Obata, M., Fujishige, M., Takeuchi, K., Wongwiriyapan, W. and Endo, M., 2020. Preparation of activated carbon via acidic dehydration of durian husk for supercapacitor applications. *Diamond and Related Materials,* 107, DOI: 10.1016/j.diamond.2020.107906.

[18] Yao, D., Hu, Q., Wang, D., Yang, H., Wu, C. and Wang, X., 2016. Hydrogen production from biomass gasification using biochar as a catalyst/support. *Bioresource Technology,* 216, 159-164.

[19] Zhang, S., Asadullah, M., Dong, L., Tay, H.L. and Li, C.Z., 2013. An advanced biomass gasification technology with integrated catalytic hot gas cleaning. Part II: Tar reforming using char as a catalyst or as a catalyst support. *Fuel*, 112, 646-653.

[20] Chang, Y.M., Tsai, W.T. and Li, M.H., 2015. Characterization of activated carbon prepared from chlorella-based algal residue. *Bioresource Technology,* 184, 344-348.

[21] Foo, K.Y. and Hameed, B.H., 2011. Microwave-assisted preparation of oil palm fiber activated carbon for methylene blue adsorption. *Chemical Engineering Journal,* 166, 792-795.

[22] Dulyaseree, P., Yordsri, V. and Wongwiriyapan, W., 2016. Effects of microwave and oxygen plasma treatments on capacitive characteristics of supercapacitor based on multiwalled carbon nanotubes. *Japanese Journal of Applied Physics,* 55(25), DOI: 10.7567/JJAP.55. 02BD05.

[23] Dresselhaus, M.S., Dresselhaus, G., Saito, R. and Jorio, A., 2005. Raman spectroscopy of carbon nanotubes. *Physics Reports,* 409, 47-99.

[24] Dresselhaus, M.S., Dresselhaus, G., Saito, R. and Jorio, A., 2010. Perspectives on carbon nanotubes and graphene Raman spectroscopy. *Nano Letters,* 10(3), 751-758.

[25] Smith, M.W., Dallmeyer, I., Johnson, T.J., Brauer, C.S., McEwen, J.S., Espinal, J.F. and Garcia-Perez, M., 2016. Structural analysis of char by Raman spectroscopy: Improving band assignments through computational calculations from first principles. *Carbon,* 100, 678-692.

[26] Guizani, C., Haddad, K., Limousy, L. and Jeguirim, M., 2017. New insights on the structural evolution of biomass char upon pyrolysis as revealed by the Raman spectroscopy and elemental analysis. *Carbon,* 119, 519-521.

[27] Faix, O., 1991. Classification of lignins from different botanical origins by FT-IR spectroscopy. *Holzforschung,* 45, 21-27.

[28] Ibrahim, M., 2002. Preparation of cellulose and cellulose derivative azo compounds. *Cellulose*, 9, 337-349.

[29] Sattayarut, V., Chanthad, C., Khemthong, P., Kuboon, S., Wanchaem, T., Phonyiem, M., Obata, M., Fujishige, M., Takeuchi, K., Wongwiriyapan, W., Khanchaitit, P. and Endo, M., 2019. Preparation and electrochemical performance of nitrogen-enriched activated carbon derived from silkworm pupae waste. *RSC Advance,* 9, 9878-9886.

[30] Wei, T., Zhang, Q., Wei, X., Gao, Y. and Li, H., 2016. A facile and low-cost route to heteroatom doped porous carbon derived from *Broussonetia papyrifera* bark with excellent supercapacitance and CO_2 capture performance. *Scientific Reports*, 6, DOI: 10.1038/srep 22646.

[31] Chen, H., Yan-chuan, G., Wang, F., Wang, G., Qi, P. and Gua, X., 2017. An activated carbon derived from tobacco waste for use as a supercapacitor electrode material. *New Carbon Materials*, 32(6), 592-599.

[32]　Du, W., Zhao, Y., Zhang, Z., Du, L., Fan, X., Shen, Z., Ren, X. and Wei, C., 2019. Designing synthesis of porous biomass carbon from wheat straw and the functionalizing application in flexible, all-solid-state supercapacitors. *Journal of Alloys and Compounds*, 797, 1031-1040.

[33]　Peng, C., Lang, S., Xu, S. and Wang, X., 2014. Oxygen-enriched activated carbons from pomelo peel in high energy density supercapacitors. *RSC Advance,* 4, 54662-54667.

[34]　Karnan, M., Subramani, K., Sudhan, N., Ilayaraja, M. and Sathish, M., 2016. Aloe vera derived activated high-surface-area carbon for flexible and high-energy supercapacitors. *ACS Applied Materials & Interfaces*, 8, 35191-35202.

[35]　Taer E., Taslim, R., Aini, Z., Hartati, S.D. and Mustika, W.S., 2017. Activated carbon electrode from banana-peel waste for supercapacitor application. *AIP Conference Proceedings*, 1801, DOI: 10.1063/1.4973093.

[36]　Fasakin, O., Dangbegnon, J.K., Momodu, D.Y., Madito, M.J., Oyedotun, K.O., Eleruja, M.A. and Manyala, N., 2018. Synthesis and characterization of porous carbon derived from activated banana peels with hierarchical porosity for improved electrochemical performance. *Electrochimica Acta*, 262, 187-196.